

(formerly WPIs) suffer from inappropriate resource and resource-type mixes].

In addition to the price of the resource, many other factors affect the cost of a job. If one views cost as output \times productivity \times resource price \times overhead, it can be seen that the price index will define one part of the cost picture. Productivity can be related to region-specific work rules and job specifications such as traffic control requirements, supply uncertainty, and weather. Overhead costs reflect market and institutional costs. Foster and others (7) identify market factors such as the bidding climate and institutional and support factors such as insurance, building permits, financing, real estate acquisition, geologic investigation, construction management, engineering design, and legal and community costs that affect the overhead rate on any job. Once the effects of price, time, and location (as represented by the transit price indices) have been determined, indices of productivity and overhead factors can be analyzed to understand costs.

ACKNOWLEDGMENT

The research for this paper was conducted as part of Transportation Systems Center work for the Office of Planning Assistance of the Urban Mass Transportation Administration to develop technical guidelines for system planning and corridor refinement studies. I wish to acknowledge the assistance of Don Ward and

Mike Jacobs in the preparation of this paper. The ideas presented here are mine and do not represent official U.S. Department of Transportation policy.

REFERENCES

1. Dodge Building Cost Services. 1979 Dodge Guide for Estimating Public Works Construction Costs, 11th annual ed. McGraw-Hill Information Systems Co., New York, 1978.
2. Means Cost Guide. R.S. Means Company, Inc., Duxbury, MA, 1978.
3. National Construction Estimator, 27th annual ed. Craftsman Book Co., Solana Beach, CA, 1978.
4. Market Trends. Engineering News Record, March 22, 1979.
5. Construction Cost Indexes for 1915-78. U.S. Department of Commerce, Construction Review, Vol. 25, No. 12, Dec. 1979.
6. Data Resources Cost Forecasting Service, Inc. Forecasting Highway Construction Costs. FHWA, Rept. FHWA-DL80-005, Feb. 1981.
7. E.L. Foster and others. Economic Factors in Tunnel Construction. U.S. Department of Transportation, Rept. UMTA-MA-06-0025-79-10, Feb. 1979.

Publication of this paper sponsored by Committee on Construction Management.

Nondestructive Monitoring of Chloride in Bridge Decks with a Mobile Neutron-Gamma Spectrometer

J.R. RHODES

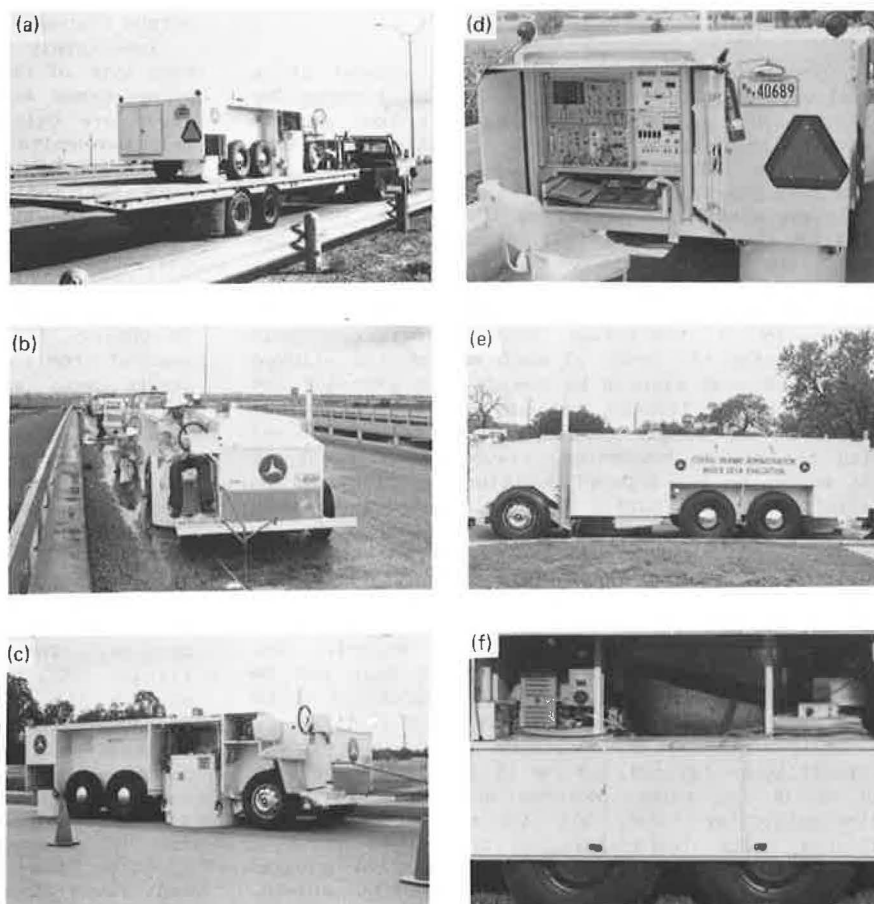
A mobile, self-contained instrument for rapid, nondestructive monitoring of chloride content at the reinforcing-bar level in portland cement concrete bridge decks has been developed to field prototype stage and tested on a range of concrete specimens and on five bridge decks in Texas. The instrument uses the technique of neutron-induced gamma-ray spectrometry with a 400- μ g californium-252 sealed neutron source. Two measuring heads provide the capability for depth discrimination and enable chloride contents to be measured at the reinforcing-bar depth irrespective of surface washout, salt encrustation, the presence of overlays or membranes, and different depth distributions of chloride content. The sensitivity to chloride obtained depends on the required depth discrimination and speed of measurement but is normally sufficient to detect chloride concentrations below the corrosion threshold of approximately 300 mg/kg (~ 1.2 lb/yd³).

The chloride-induced deterioration of reinforced portland cement concrete (PCC) is one of the most important problems currently facing the highway industry (1). All PCC bridge decks to which deicing salts have been applied and all PCC structures exposed to sea salts are susceptible. As little as 300 mg/kg (~ 1.2 lb/yd³) of chloride ion counteracts the passivity of the steel reinforcing and allows electrochemical corrosion to proceed rapidly. The onset of rapid corrosion can be very difficult to detect because the depth distribution of chloride concentration can vary due to factors such as surface washout or accumulation of salt and because the concrete surface may have been covered with a protective overlay or membrane.

In addition to membranes and asphalt overlays, other materials impermeable to chloride are being used both at repair sites and in new construction. Any test method should be capable of monitoring chloride content without interference from any of the materials used in bridge decks. The present test method is to remove pulverized core samples taken at various depth increments by means of a rotary hammer and to analyze them in the laboratory by using a wet chemistry-potentiometric technique. This method is time consuming, labor intensive, and traffic disrupting. Its destructive nature makes it unsuitable for sampling below impermeable membranes and requires refilling of the sample holes. Furthermore, because of the small sample size and the heterogeneity of concrete, more samples than might otherwise be needed have to be taken to yield a survey of acceptable accuracy (1).

The main objective of the project described here was to develop a field instrument and test procedure for rapid, in situ, nondestructive determination of chloride ion content in PCC bridge decks and other reinforced concrete members at the level of the outermost mat of reinforcing steel. A detailed feasibility study (2) resulted in the choice of neutron-induced gamma spectrometry as the preferred method of measurement. The unique advantage of neutron-gamma spectrometry is that the incident neutrons and emitted characteristic gamma rays have

Figure 1. Prototype bridge-deck analyzer: (a) on flatbed trailer, (b) being positioned, (c) measuring heads in position on road surface, (d) instrumentation panel at rear, (e) left-hand side of vehicle, and (f) support systems.



ranges of several centimeters in solids, thus permitting representative analysis of coarse bulk materials and offering the possibility of nondestructive depth chloride determinations. A dual neutron-gamma measurement procedure was conceived and demonstrated experimentally to yield independent "surface" and "depth" chloride content determinations on PCC test specimens. Two measuring heads were designed, each of which has a different depth sensitivity. A prototype field instrument has been developed that incorporates the two measuring heads and provides all support systems necessary for semiautomatic, mobile field operation. In addition to real-time monitoring of bridge decks, the bridge-deck analyzer can be used for rapid chloride content determination of small [300-g (0.6-lb)] pulverized concrete samples and for multielement analysis of large [200- to 500-kg (440- to 1100-lb)] samples of coarse [minus 5-cm (minus 2-in)] bulk materials.

This paper describes the instrument and summarizes the results obtained in laboratory and preliminary field trials. Full details are reported elsewhere (3).

DESCRIPTION OF INSTRUMENT

General

The prototype bridge-deck analyzer shown in Figure 1 is a self-propelled vehicle that weighs 4300 kg (5 tons) and measures 1.44 m high by 5.64 m long by 1.98 m wide (4.75x18.5x6.5 ft). It is designed to be driven from one measurement spot to the next, but for analyses to be made the vehicle must be stationary and the measuring heads lowered hydraulically onto the surface of the material. The vehicle

is moved long distances on a suitable transporter, such as a flatbed trailer, as shown in Figure 1a. Figure 1b shows the vehicle being positioned for a measurement. Note the fold-away pointer extended to aid accurate positioning. When extended, the pointer is 3.05 m (10 ft) in front of the axis of the forward (prompt-gamma) measuring head, which is itself 3.05 m in front of the axis of the rear (activation-gamma) measuring head. The pointer and the measuring-head axes are on the same straight line running fore and aft. Figure 1c shows both measuring heads lowered to the road surface for a dual neutron-gamma depth chloride measurement.

Figure 1d shows the instrumentation panel at the rear and the demountable operator's seat and "umbrella". Figure 1e shows the left-hand side of the vehicle. The forward cupboard has about 1 m³ (35 ft³) of storage space. The fold-down door gives access to the support systems (on-board power and temperature-controlled air and water), which are shown in Figure 1f.

Nuclear Instrumentation

The nuclear instrumentation comprises (a) a prompt-gamma measuring head, which is also the irradiator for the activation-gamma measurement and the source storage chamber; (b) an activation-gamma measuring head; and (c) a gamma-ray spectrometer interfaced to a small computer with cassette tape storage and printer and to a data sequencer. During semiautomatic operation, six buttons with integral indicator lights on the data sequencer lead the operator through the measuring sequence and prevent acquisition of erroneous data, or improper source exposure, through various interlocks.

Measuring Heads

The prompt-gamma measuring head is housed in a steel-walled cylinder 0.9 m (3 ft) in diameter by 0.9 m high that weighs 1080 kg (0.5 ton) and is filled with neutron and gamma-ray shielding material. The 400- μ g californium-252 source (half-life 2.65 years) is encapsulated in a solid, welded, stainless steel cylinder, 1 cm (0.4 in) in diameter by 3 cm (1.2 in) long, that moves up and down the axis. The "home" position of the source is at the center, and the "exposed" position is 2.5 cm (1 in) from the base. The source movement mechanism is driven by a reversible stepper motor. Limit switches stop the motor at each end of the allowed travel and send signals to the "source exposed" and "source home" lighted buttons on the data sequencer. The sample contact switch is interlocked with the source mechanism, preventing movement of the source to the exposed position and lighting the "shield not down" button on the data sequencer when the prompt-gamma head is not in contact with the sample. Additional visual indication of the source position is provided in the form of the color of the source retraction chain visible to the operator: red for exposed and green for home. In addition, a Klaxon sounds when the source is moving. The neutron shield has a movable segment that can be raised by a hand crank to enable measurements to be made as close to roadside curbs as 31 cm (1 ft).

The prompt-gamma-ray detector is a sodium iodide scintillation crystal, 13 cm (5 in) in diameter by 10 cm (4 in) thick, mounted on a 13-cm-diameter photomultiplier tube, all in a light-tight enclosure. The temperature is controlled to $\pm 1^\circ\text{C}$ ($\pm 33.8^\circ\text{F}$). The whole subassembly is shock mounted inside the gamma-ray and thermal neutron shield. The source-detector geometry is optimized to provide maximum sensitivity to depth chloride for least cost in terms of signal-to-background ratio. The measurement cannot be made insensitive to surface chloride.

The activation-gamma measuring head comprises a temperature-controlled, shock-mounted detector assembly identical to that in the prompt-gamma head, all housed in a cylindrical steel-walled shield 0.61 m (2 ft) in diameter by 0.43 m (17 in) high that weighs 360 kg (800 lb). The activation measurements are optimized to provide maximum sensitivity to surface chloride and minimum response from depth chloride.

Gamma-Ray Spectrometer

The gamma-ray spectrometer is housed in a custom-built NEMA 4 specification instrument cabinet that is air conditioned and temperature controlled to $24^\circ \pm 8^\circ\text{C}$ ($75^\circ \pm 14^\circ\text{F}$). The rack containing the multichannel analyzer (MCA) and electronic modules (the left-hand panel in Figure 1d) is covered by a plexiglas door, which prevents access during routine operation to every module except the data sequencer (top right in Figure 1d) and the electrical panel (bottom right). The electrical panel contains the switches and meters for the electrical supplies and detector temperature monitoring.

The spectrometer operates as follows. Gamma rays absorbed in the sodium iodide crystal produce light scintillations that are seen by the photomultiplier, converted into electrical charge pulses, and amplified by linear pulse amplifiers whose output pulses have voltages proportional to the original energies of the gamma rays. The MCA sorts the pulses into channels according to their voltages and accumulates each gamma-ray spectrum as a histogram of number of pulses per channel in a given measurement time

versus channel number (i.e., gamma energy).

Immediately after absorbing a thermal neutron, each type of nuclide in the sample emits a group of prompt-gamma rays. The energies and number in the group are uniquely characteristic of the nuclide. Chlorine emits many prompt gammas in the energy range 3-9 MEV, and they are only partly resolved from all the other prompt gammas. In fact, a prompt-gamma spectrum is characterized by having a large number of gamma-ray peaks from a relatively small number of components in the sample.

Activation-gamma rays are emitted as a result of the decay of thermal-neutron-induced radioactivity. To observe these gamma rays, the sample is first removed from the source (or vice versa) to stop the prompt-gamma emission and eliminate the neutron background. Because the thermal neutron activation cross sections of Mn, Na, Al, and Cl are very high, their gammas predominate even at low concentrations of these elements. In contrast, H, C, O, Si, and Fe are not activated by thermal neutrons. The activation-gamma spectrum has fewer peaks than the prompt-gamma spectrum, but the problem of resolving the chlorine gammas remains.

Various methods of mathematical analysis have been used to deconvolute partly resolved gamma spectra. The method used here is least-squares fitting (LSF) of library spectra (4, p. 193). Gamma spectra are obtained for each and every uniquely characterized component of the material to be analyzed and are stored in a library (on a tape cassette in this case). Analysis then proceeds on the assumption that the "unknown" spectrum is a linear combination of the library spectra. The fraction of each library component in the unknown spectrum is assumed to be proportional to the concentration of that component in the material being analyzed. The values of these fractions are found by using the least-squares method to calculate the best fit of the library spectra to the unknown spectrum.

Support Systems and Accessories

The instrument is propelled by a front-wheel-drive automobile engine complete with drivetrain, automatic transmission, and front suspension. The driver's station (Figures 1b and 1c) consists of a seat, steering wheel, instrument console, gear-shift lever, and brake and accelerator pedal. The driver's station is placed over the right-front wheel directly above the line that joins the centers of the two measuring heads and the pointer.

The power required for the electronic instrumentation, the heater and cooler for instrument air, and the heater and cooler for detector temperature control fluid is 110 V alternating current (ac). This is provided by a wall socket when available or by an on-board 4-KVA motor generator in the field. The pump for the detector temperature control fluid is powered by 12 V direct current (dc) so that fluid can be kept circulating at all times, particularly while the vehicle is being transported from site to site. The automotive car battery powers the pump as well as the rest of the 12-V dc system (ignition and lights). The battery is charged either from the 110-V ac system or by the automotive alternator.

Each measuring head is suspended from four hydraulic jacks and can be raised and lowered independently by using two levers in the hydraulic station directly behind the driver's seat. The hydraulic system is operated from a pump mounted above the automotive engine. A manually operated pump is also provided to obtain hydraulic pressure in the event of power failure. Sample holders in the form of dollies are provided for holding cali-

Table 1. Definitions of calibration models.

Model	Description	C_s	C_d	Expected Precision (mg/kg)	
				ΔC_s	ΔC_d
B	Uniform for first 1.3 cm exponential in range 1.3-7.6 cm; zero below 7.6 cm	Avg in 0- to 1.3-cm depth increment	Value at 5.1 cm below surface	630	66
D	Uniform chloride distribution	-	Avg in 0- to 15-cm depth increment	-	38

Note: 1 cm = 0.39 in; 1 mg/kg = ~ 0.004 lb/yd³.

bration standards, concrete test specimens, and bulk materials.

Dual-Measurement Procedure

A dual measurement is required to determine chloride content at a given depth below the surface. Dual measurements are made along a straight line at pre-marked spots 3.05 m (10 ft) apart. The instrument is driven along the line until the extended pointer is over the second spot to be measured. The prompt-gamma measuring head is then over the first spot. This head is lowered, and the prompt-gamma measurement made. The head is then raised, the instrument is driven forward until the pointer is over the next spot, and both heads are lowered. The activation-gamma head then makes its measurement on the first spot while the prompt-gamma head is measuring and irradiating the second spot. The two readings for each spot are combined by applying them to a simultaneous linear equation to yield depth and surface chloride concentrations. The usual measurement time is 10 min with a 5- to 10-min delay period in between. Results are printed out about 5 min after the second measurement of each spot, and an average of 3 spots/h are measured.

Single-Measurement Procedure

In the single-measurement mode, only the prompt-gamma head is used and the chloride concentrations obtained are weighted depth averages of the total chloride in the deck. The measurement spots need be neither on a straight line nor 3.05 m (10 ft) apart. At least 6 spots/h can be measured in this mode.

EXPERIMENTAL RESULTS

Laboratory measurements were made on more than 100 test specimens to assess the effects on the chloride reading of changes in concrete composition, reinforcing bars, overlays and membranes, and chloride concentration gradients. The test specimens were mixed, cast, and cured by using standard procedures, and some of them were analyzed by using the standard method of sampling and wet chemistry. Field trials were conducted on five bridges in Texas that were chosen to yield experience on a range of bridge types, deck conditions, salting histories, and geographic locations.

Laboratory Measurements on Specimens with Uniform Chloride Content

Some 122 prompt- and activation-gamma readings were

made on test specimens that covered variations in chloride concentration [0-3000 mg/kg (0-12 lb/yd³)] aggregate (eight widely varying types were tested), water/cement (w/c) ratio (0.45-0.65), free-water content (0-5 percent), reinforcing-bar pattern and depth, and presence of overlays and membranes. The overlays tested included polymer concrete, asphalt concrete, wax-bead-loaded PCC, and latex-modified PCC. In addition, typical asphaltic membranes were inserted between the asphalt concrete overlay and the PCC specimen.

The activation- and prompt-gamma methods each gave a linear response over the full range of chlorine content. No significant interferences were found due to variations in aggregate type or maximum particle size; w/c ratio or free-water content; reinforcing-bar presence, pattern, or depth; or, with one exception, the presence of overlays and membranes. Two polyvinyl chloride (PVC) materials, Dow Latex B overlay and Superseal 4000 membrane, gave very large signals when measured with a zero-chloride test specimen. This is to be expected since PVC is mainly chlorine.

Nonuniform Chloride Content

Unknown chloride concentration distributions are handled by the dual-measurement procedure, which can, by solution of a pair of simultaneous equations, determine the chloride content at two specific depths below the surface of a bridge deck. One of these is the reinforcing-bar depth, which is usually 5.1 cm (2 in) but can be as little as 2 cm (0.75 in) for a worn deck and 10-15 cm (4-6 in) for an overlaid deck. The chloride content at the reinforcing-bar level is defined as the depth chloride (C_d); the second variable is the surface chloride (C_s). A calibration model must be defined that specifies the depth or depth increment for C_s and C_d and states the assumptions to be made about the chloride concentration distribution. There are an infinite number of such models, but the most useful ones can be chosen by taking into account our knowledge of real chloride concentration distributions and of the depth sensitivity profiles of each neutron-gamma measurement. The sensitivity of the prompt-gamma measurement falls off slowly from the surface down to about 20 cm (8 in), below which it is essentially zero. The sensitivity of the activation-gamma measurement falls off rapidly and is zero below about 4 cm (1.6 in) from the surface.

The chloride concentration distribution is only important in the sensitive ranges of the neutron-gamma measurements. In controlled experiments, Clear (5) obtained exponential distributions with varying gradients. The average gradient was a factor of two per 1.3-cm (0.5-in) depth increment. On real bridge decks, the first 5 mm (0.2 in) or so of a nonoverlaid deck can have any chloride content, independent of the distribution at greater depths, because of the possibility of surface washout or salt encrustation. Overlays present an additional thickness of 1-10 cm (0.5-4 in), which is usually chloride free.

Several calibration models were tested. The results for the two most promising models, B and D, are given here. Table 1 describes each model, defines C_s and C_d , and gives the expected precisions (ΔC_s and ΔC_d).

The instrument was calibrated for each model by measuring stacks of test specimens that had known chloride contents and concentration distributions that corresponded to the models as defined. The results were used to calculate the calibration coefficients, which are the coefficients of the pair of

simultaneous linear equations relating C_s and C_d with the responses, I_1 and I_2 , of each measuring head.

The expected precisions were calculated by substituting the measured values, ΔI_1 and ΔI_2 , of instrument repeatability into the pair of simultaneous linear equations relating ΔC_s and ΔC_d with ΔI_1 and ΔI_2 . Repeated measurements of test specimens revealed that ΔI_1 and ΔI_2 are independent of any of the sample variables and are constant for a given source strength and measurement time sequence. The differences in ΔC_s and ΔC_d between models are the result of each model having a different set of coefficients. Better precision and sensitivity are traded for reduced depth "resolution".

Laboratory Measurements of Nonuniform Chloride Content

Table 2 gives a selection of the results for the two models, obtained for measurements on 1.3-cm (0.5-in) thick test specimens stacked to simulate various chloride concentration distributions and concrete compositions. These include the average Clear exponential distribution with and without surface washout and salt encrustation as well as overlays, reinforcing bars, and different water contents. Model B is very successful at eliminating effects on C_d due to high surface chloride concentrations (see samples 1, 3, 5, 8, 9, and 13). Model D, which requires only a single prompt-gamma measurement, is clearly a practical proposition for rapid screening. The model tends to overestimate the value of C_d , especially when the chloride is near the surface, but this can be corrected by a change in the calibration coefficient. The results for specimen stacks 10-14 illustrate the ability of each model to avoid "false positive" readings. Stack 10 yields results that are representative of all the non-PVC overlays and membranes tested. No model gave a C_d reading more than about ± 1 standard deviation different from zero. Stack 11 is representative of all of the different reinforcing-bar patterns and

depths. No model gave an error in C_d greater than ± 2 standard deviations. Stack 12 is representative of all w/c ratios and free-moisture contents. Again, no error was greater than ± 2 standard deviations. The effects of the PVC overlay and PVC membrane are shown in entries 13 and 14. Considering that the chlorine content of these materials is orders of magnitude greater than the range of interest for corrosion in bridge decks, the errors caused by them are small.

The effects of overlays 1.3-7.6 cm (0.5-3 in) thick are given in Table 3. The expected and measured values of C_s and C_d were recalculated for six specimen stacks after the surface and depth chloride concentrations were redefined as measured from the base of the overlay rather than the surface of the specimen. It is seen that model B tends to underestimate C_d for large overlay thicknesses whereas model D shows good agreement for thick overlays. Prior knowledge of the approximate overlay thickness would eliminate these errors.

Field Trials on Bridge Decks

Approximately 50 nondestructive neutron-gamma measurements were made on each of five bridges by using the dual- and single-measurement procedures described earlier. Conventional chloride determinations were made by sampling approximately one-third of the nondestructive measurement sites. The instrument operated reliably in moderate rainfall, but samples could not be taken in these conditions. The iron signal from steel beams was found to be much greater than that from reinforcing bars, but the data analysis procedures successfully handled this.

Analysis of the rotary hammer samples showed that in all but one case the assumption concerning exponential depth chloride distribution was supported. However, the exponents varied from $-0.2x$ to $-0.4x$ with an average value of approximately $-0.3x$ (where x is depth in centimeters), which is at variance with the assumption of $-0.6x$ on which the calibration for model B is based. The results for C_d were corrected for this. In addition, the wet

Table 2. Measurements on concrete specimens.

Description of Specimen Stack ^a	Chloride (mg/kg)					
	Model B				Model D	
	Measured		Expected			
	C _s	C _d	C _s	C _d	Measured	Expected
5000, 450, 210, 100, 50, 20 mg/kg Cl; rest 0	5 090	109	5000	75	824	486
0, 450, 210, 100, 50, 20 mg/kg Cl; rest 0	-1 104	234	0	75	249	69
5000, 1900, 900, 420, 210, 100 mg/kg Cl; rest 0	5 960	237	5000	315	1147	711
0, 1900, 900, 420, 210, 100 mg/kg Cl; rest 0	720	256	0	315	516	294
5000, 4000, 1900, 900, 420, 210 mg/kg Cl; rest 0	6 490	402	5000	660	1490	1036
0, 4000, 1900, 900, 420, 210 mg/kg Cl; rest 0	-720	632	0	660	960	619
1900, 900, 420, 210, 100, 50 mg/kg Cl; rest 0	3 570	109	1900	155	633	298
4000, 1900, 900, 420, 210, 100 mg/kg Cl; rest 0	5 870	293	4000	315	1229	628
5000 mg/kg Cl; rest 0	5 120	-2	5000	0	644	417
2.5-cm asphalt overlay; all 0	-18	-25	0	0	-45	0
Rebar at 4.5 cm, all 0	-448	-7	0	0	-69	0
All 0, any w/c or moisture	-29	5	0	0	5	0
2.5-cm PVC modifier overlay; rest 0	27 700	258	High	0	3924	High
0, 0, Superseal 4000 PVC membrane; rest 0	-1 398	810	High	0	1170	High

Note: 1 mg/kg = ~ 0.004 lb/yd³; 1 cm = 0.39 in.

^aChloride listed in successive 1.3-cm (0.5-in) depth increments from surface.

Table 3. Effects of overlays.

Description of Specimen Stack ^a	Chloride (mg/kg)					
	Model B					
	Measured		Expected		Model D	
	C _s	C _d	C _s	C _d	Measured	Expected
450, 210, 100, 50, 20 mg/kg Cl; rest 0 ^b	-1104	110	450	35	249	69
1900, 900, 420, 210, 100 mg/kg Cl; rest 0 ^b	720	120	1900	155	516	294
420, 210, 100 mg/kg Cl; rest 0 ^c	-110	19	420	0	163	61
450, 210, 100, 50, 20 mg/kg Cl; rest 0 ^d	-1680	9	450	35	82	69
1900, 900, 420, 210, 100 mg/kg Cl; rest 0 ^d	-2870	20	1900	155	317	294
4000, 1900, 900, 450, 210, 100 mg/kg Cl; rest 0 ^e	-4580	8	4000	330	686	630

Note: 1 mg/kg = ~0.004 lb/yd³.^aChloride listed in successive 1.3-cm (0.5-in) depth increments from surface.^bAll under 1.3-cm overlay.^cAll under 3.8-cm (1.5-in) overlay.^dAll under 5.1-cm (2-in) overlay.^eAll under 7.6-cm (3-in) overlay.

Table 4. Sample volumes and sampling errors.

Method	Effective Volume Sampled (cm ³)	Sampling Error ^a (%)
Neutron-gamma	5000	0.6
Core sample, 10 cm diameter x 2.5 cm deep	210	8.4
Rotary hammer sample, 3.8 cm diameter x 1.3 cm deep	15	32

Note: 1 cm³ = 0.061 in³; 1 cm = 0.39 in.^aCoefficient of variation.

Table 5. Comparison of average chloride contents for five bridge decks.

Bridge	Chloride (mg/kg)			
	Neutron-Gamma			
	Model B			
	C _s	C _d	Model D	Sampling Plus Wet Chemistry
1	130	57	73±73	105±44
2	2090±1809	686±343	575±261	542±326
3	2401±1855	797±602	664±284	873±545
4	5339±2182	395±432	638±273	490±389
5	563±124	43±35	54±38	111±14

Note: 1 mg/kg = ~0.004 lb/yd³.

corresponding sampling errors were calculated by using particulate sampling theory (6). The relative standard deviation of a single rotary hammer sample is 32 percent.

Comparisons of average chloride contents for the five bridges yielded by the conventional and neutron-gamma measurements are summarized in Table 5. These comparisons must of necessity be semiquantitative because of the variability of the chloride distributions and the noncorrespondence between the volumes sampled by each method and the sites measured by each method. Even though the relative standard deviations vary from 13 to 109 percent, semiquantitative agreement between most of the mean values is quite good. The results for model D are especially interesting, since this model uses only one measuring head and can monitor with twice the sensitivity and at twice the rate of the dual method. Detailed results of the field trials are given elsewhere (3).

CONCLUSIONS

The mobile bridge-deck analyzer shows promise of being able to evaluate bridge decks far more rapidly and economically than the conventional methods. Fewer measurements are required for equivalent quality of data. Each measurement is faster and decisions can be made to optimize measurement patterns on the basis of real-time results. Although the capital cost of the instrument is high, its operating costs are low and, with good planning, amortization can be spread over thousands of bridge decks. One technician-grade operator with one assistant (plus flagmen, as required by the location) could operate the instrument after suitable training.

ACKNOWLEDGMENT

I wish to acknowledge the support of the 24 state highway agencies that sponsored this work and whose representatives directed it. I would also like to express appreciation for the encouragement and guidance of T.M. Mitchell of the Federal Highway Administration and for the work done by N.J. Carino of the National Bureau of Standards (formerly at the University of Texas) in preparing the concrete test specimens and J. Canfield of the Texas State Department of Highways and Public Transportation in helping to organize the field trials. Last but not

chemistry results were corrected where necessary to a 5.1-cm (2-in) depth to allow comparison with the neutron-gamma measurements.

Chloride in PCC bridge decks does not penetrate the coarse aggregate but is distributed throughout the mortar. This causes the well-known "aggregate-induced distortion" (1), a local heterogeneity that is present even when the average chloride content is uniform on a large scale. Sampling errors caused by this can be very great when the sample size is similar to the volume of a coarse aggregate particle, as is the case with rotary hammer samples. Sampling errors can be reduced by making sample volumes so large that local fluctuations in coarse aggregate concentration become negligible. Table 4 gives the effective sample volumes of the neutron-gamma methods and the volumes of standard cores and rotary hammer samples. It can be seen that some 330 rotary hammer samples would be required to give the same sample volume as the neutron-gamma method. The

least, I wish to acknowledge the untiring efforts of my associates, J.A. Stout, J.S. Schindler, and R.D. Sieberg, in assembling and operating the instrument.

REFERENCES

1. Durability of Concrete Bridge Decks. TRB, Synthesis of Highway Practice 57, 1979.
2. J.R. Rhodes and others. In Situ Determination of the Chloride Content of Portland Cement Concrete in Bridge Decks: Feasibility Study. FHWA, Interim Rept. FHWA-RD-77-26, 1977.
3. J.R. Rhodes and others. In Situ Determination of the Chloride Content of Portland Cement Concrete Bridge Decks. FHWA, Final Rept. FHWA-RD-80-030, 1980.
4. L. Salmon. Analysis of Gamma Ray Scintillation Spectra by the Method of Least Squares. Nuclear Instruments and Methods, Vol. 14, 1961.
5. K.C. Clear. Time to Corrosion of Reinforcing Steel in Concrete Slabs: Volume 3--Performance After 830 Daily Salt Applications. FHWA, Interim Rept. FHWA-RD-76-70, 1976.
6. C.L. Grant and P.A. Pelton. Role of Homogeneity in Powder Sampling. ASTM, Philadelphia, Special Tech. Publ. 540, 1973, pp. 16-29.

Publication of this paper sponsored by Committee on Instrumentation Principles and Applications.

Development of an Improved Automated Nuclear Backscatter Gage

RAYMOND A. FORSYTH, FRANK C. CHAMPION, AND JOSEPH B. HANNON

The design, construction, and evaluation of a prototype automated vehicle-carried nuclear moisture-density backscatter gage are described. Gage development was based on research and analysis concerning several factors that affect gage performance. This research indicated that the prototype backscatter-gage measurements were approximately equivalent to measurements obtained by commercial transmission gages. The implication of this research finding is the possibility of a backscatter test method as a valid, reliable, and expedient procedure for determining in situ soil conditions. Field comparisons between the prototype gage and a commercial nuclear backscatter gage demonstrated a marked improvement in performance by the prototype gage. The prototype gage is installed in a motor vehicle together with a hydraulically operated mechanism that automatically positions the gage for testing. The vehicle gage unit, or Autoprobe, can determine in situ moisture and density values in 3 min. The Autoprobe is now ready for use by the California Department of Transportation for investigational and quality-control purposes.

The work reported in this paper was the outgrowth of three separate, but interrelated, federally funded research projects that were carried out simultaneously. The first resulted in the development of nuclear gage standards for calibration and evaluation of gage performance (1). In the second project, various elements of nuclear gage performance were explored for the purpose of developing meaningful specifications for the purchase of nuclear gages (2). The objective of the third project, which is reported on here, was the development of a backscatter gage that would equal or exceed the performance of approved direct-transmission gages. The principal advantage of the backscatter mode of testing is that both the source and the detector remain at the surface, which eliminates the need for an access hole into the test material. The obvious benefit is a faster and simpler test, which allows more tests in a given time period.

Currently, the transmission mode is considered to be the most accurate and reliable method of nuclear density testing. The transmission technique, which requires insertion of the gamma source into the test material, has proved to be less affected by surface conditions and more sensitive to density changes. It also tests a larger volume of compacted materials due to gage configuration.

Previous analyses by California Department of Transportation (Caltrans) researchers of the factors that affect nuclear moisture-density gage measurements have been limited to investigations of the difficulties encountered under field conditions. Factors such as surface roughness, air gaps, and gage calibration methods were among the items investigated. The present project began with an evaluation of the basic commercial nuclear gage, including the characteristics of the backscatter and direct-transmission modes of operation. The paper describes the subsequent development of an optimized prototype backscatter gage. More detail is available in reports by Chan and others (3) and Champion and others (4).

DEVELOPMENT OF PROTOTYPE GAGE

General Considerations

During the development of the prototype backscatter gage, various interrelated gage features that have significant effect on gage performance were studied. These included the geometric relation between the radioactive source, the test material, and the radiation detector. The backscatter mode involves measurement of attenuated gamma-ray emissions deflected to and from the test medium surface. Thus, the distance separating the radioactive source and the radiation detector is a primary factor in gage performance. In the transmission mode, the radioactive source is lowered into the test medium while the detector remains at the surface.

Second, the detection of particular attenuated gamma-ray energies has a marked effect on gage performance. Each source has its own characteristic energy spectrum. Attenuation of the spectrum by the test medium produces a wider variation of low-energy gamma rays than originally emitted by the source. Detection of low energies is undesirable due to absorption effects of the test materials, which vary with the mineral composition of the soil. Consequently, this parameter was carefully examined to